Effect of on-site Coulomb repulsion term U on the band-gap states of the reduced rutile (110) TiO_2 surface

Carmen J. Calzado,* Norge Cruz Hernández, and Javier Fdez. Sanz
Departamento de Química Física, Facultad de Química, Universidad de Sevilla, E-41012 Sevilla, Spain
(Received 26 October 2006; revised manuscript received 31 July 2007; published 15 January 2008)

We present a study concerning the effect of the on site d-d Coulomb interaction energy U on the band-gap states of nonstoichiometric rutile (110) TiO_2 surface. As well known, the excess electrons resulting from the formation of oxygen vacancies localize on the Ti $3d$ orbitals forming band-gap states. Local density approximation (LDA) does not give a correct description of these band-gap states, either with or without gradient corrections. The failure of LDA is often attributed to an inadequate treatment of electron correlation in systems with localized orbitals and is commonly corrected with an empirical local Coulomb repulsion term, i.e., the LDA+U method. This study provides a completely general strategy to estimate the U value in this kind of systems, illustrated here for reduced (110) TiO_2 surface, well characterized from experiments. From *ab initio* embedded cluster configuration interaction calculations, combined with the effective Hamiltonian theory, a value of U of 5.5±0.5 eV is obtained, in good agreement with those reported for this system from x-ray photoemission spectroscopy experiments (U=4.5±0.5 eV). It is observed that when the *ab initio* estimate of U is injected into the periodic LDA+U calculations, a correct description of the gap states is obtained from the periodic LDA+U calculations. Additionally, the results indicate that the position of these states on the band gap strongly depends on the level at which lattice relaxation is taken into account, with significant differences between the density of states curves at the LDA+U level obtained using the optimal generalized gradient approximation or LDA+U geometries. These results suggest that this combined strategy could be a useful tool for those systems where electron correlation plays a key role, and no experimental data are available for the on-site Coulomb repulsion.

DOI: 10.1103/PhysRevB.77.045118 PACS number(s): 71.15.Mb, 31.15.V−, 31.15.A−

I. INTRODUCTION

Titanium dioxide is probably one of the most studied compounds in material science, due to its versatility and large range of applications from white pigments to catalyst support (Ref. 1 and references therein). Together with the improvement of the experimental techniques, the knowledge of this material has taken benefit of the development of sophisticated theoretical approaches, which have helped in understanding the structure and reactivity of TiO_2 surfaces.

Since most of the real applications deal with substoichiometric TiO_2, there has been an increasing effort in characterizing both the geometrical and electronic structures of reduced TiO_2, specially the rutile (110) surface which is the most stable.[2]

Reduction can be induced by removal of oxygen atoms as well as by deposition of alkali metal atoms. Both processes produce Ti^{+3} ions and localized band-gap states formed by Ti $3d$ orbitals.[1] Different spectroscopic techniques support this description such as ultraviolet photoemission spectra (UPS),[2–4] resonant photoemission,[5–7] electron energy loss spectroscopy (EELS),[8,9] or x-ray photoelectron spectroscopy.[6] Indeed all these features disappear after adsorption of molecular oxygen at room temperature. The defect states lie in the upper half of the gap, 0.75–1.18 eV below the conduction-band minimum,[10] although their position depends on the vacancy concentration, moving toward the conduction band as the defect concentration increases. Also broad peaks have been observed in the region of 450–750 nm, attributed to defect levels due to oxygen vacancies, placed at about 2 eV below the conduction-band edge.[11–14] However, Henderson *et al.*[15] have recently proposed an alternative assignment of these peaks based on Franck-Condon arguments. They considered that these peaks can correspond to excitations from electron trap states located at about 1 eV below the conduction-band (CB) edge to Ti $3d$-derived levels placed at 1 eV above the CB edge, where See and Bartynski[16] have situated the first maximum in Ti $3d$ density of states.

In the past years these band-gap states have renewed the interest in this material since they enhance the photocatalytic activity observed in titanium oxide on several processes such as the degradation of organic pollutants in water (Ref. 17 and references therein) or the solar energy conversion.[18,19] The presence of these defect states reduces the energy needed for photoexcitation with respect to the stoichiometric material, making possible the use of visible light, which opens the way to low-cost applications.

There have been previous theoretical studies of the reduced (110) surface of TiO_2 focusing on the band-gap states. Most of them predict that Ti $3d$-derived conduction-band states become occupied after reduction, but in general they fail in the position of these new states. Among those using periodical approaches we can mention the work by Ramamoorthy *et al.*,[20] in which using plane-wave pseudopotential techniques based on local density functional approximation (LDA) they found Ti $3d$-like surface states but lying in the conduction band. The same result has been obtained from spin polarized calculation performed by means of the full-potential linear muffin-tin orbital method by Paxton and Thiên-Nga.[21] Lindan *et al.*[22] using gradient corrections to the local density approximation and spin polarized calculations

show results which are qualitatively correct but the band-gap states are too close to the conduction-band edge. As far as we know, the best theoretical description of these states has been recently provided by Di Valentin *et al.*,[23] achieved only when the lattice distortion induced by the extra electrons is accounted for with the Becke 3-parameter Lee-Yang-Parr (B3LYP) functional.

The failure of pure density functional methods [LDA or generalized gradient approximation (GGA)] could be associated with an inadequate description of the strong Coulomb interaction between 3*d* electrons localized on Ti atoms. This could be corrected by introducing an additional term *U*, which takes into account the repulsion between two electrons placed on the same 3*d* orbital. This approach, named LDA $+U$ (or GGA$+U$) method, has provided descriptions in a reasonable agreement with experiments for systems where LDA solutions where systematically wrong, such as the EELS spectra of nickel oxide.[24]

However, the main limitation of this method is that *U* is conceived as an empirical term, which is varied until convergence with the experimental results. Many examples of the application of this pragmatic approach can be found in literature. A very recent one is the work by Loschen *et al.*[25] dedicated to the study of the electronic structures of CeO_2 and Ce_2O_3. This procedure is not comfortable, especially when experimental *U* values are not available, and it is not possible to check whether the *U* value giving the correct answer is or not physically meaningful. An alternative to this trial-and-error procedure is the method proposed by Cococcioni and de Gironcoli[26] to determine *U* in a self-consistent way. However, while quite promising for some systems, its success is not universal. For instance, the application of this method to the study of the electronic structure of CeO_2 provides *U* values which are underestimated with respect to the optimal *U* value,[27] while overestimated *U* values have been obtained for iron heme complexes.[28] In this context, any independent evaluation of *U* previous to the LDA$+U$ calculations would be desirable, and this is the aim of the present work.

We report on a general strategy combining *ab initio* embedded cluster calculations and effective Hamiltonian theory which yields estimates of the on-site Coulomb repulsion term. This value is later injected on the periodic LDA$+U$ calculations and provides, as will be discussed below, a correct description of the band-gap states of reduced (110) TiO_2 surface as well as their dependence on the vacancy concentration. It is worth to note that TiO_2 is one of the simplest of the systems where electron correlation could play a crucial role on the description of the electronic structure. It has been chosen as an illustrative example since there is a vast amount of available experimental data which permit us to check the validity of our procedure. The whole strategy, however, is completely general and can be extended to systems containing more than one *d* electron per site.

The paper is organized as follows. Section II presents the methodology to obtain *U* from *ab initio* embedded cluster calculations, as well as the computational details of the periodic LDA$+U$ calculations. Section III discusses the results and Sec. IV contains the main conclusions from this work.

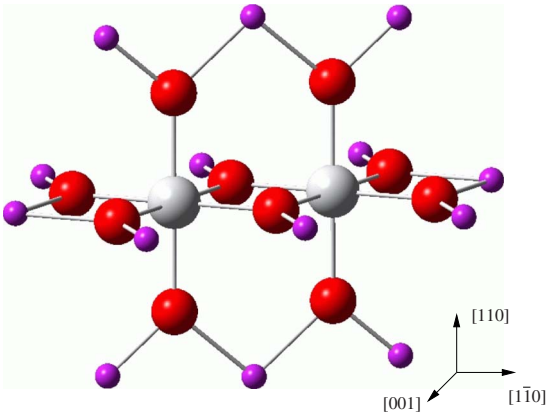

FIG. 1. (Color online) Ti_2O_{10} fragment used in *ab initio* embedded cluster calculations. Gray and large dark spheres correspond to Ti and O atoms, respectively. Ti total ion potentials (TIPs) are represented as small dark spheres.

II. COMPUTATIONAL STRATEGY

A. *Ab initio* embedded cluster calculations

1. Evaluation of U from ab initio embedded cluster calculations

The on-site Coulomb repulsion *U* for reduced TiO_2 has been determined from *ab initio* embedded cluster calculations. When TiO_2 is reduced by creating oxygen vacancies or by the deposition of alkali metals, the electron excess localizes on Ti 3*d* orbitals. Let us consider a fragment of the reduced TiO_2 system, containing two neighbor Ti centers (Fig. 1) each of them with one 3*d* electron. Let us call *a* and *b* the 3*d* occupied orbitals placed at Ti_A and Ti_B centers, respectively. Three different situations can be conceived for these two electrons in two orbitals:

(1) one electron per orbital, with opposite spins, represented by the determinants $|a\bar{b}|$ and $|b\bar{a}|$;

(2) one electron per orbital, with parallel spins, that is, the determinants $|ab|$ and $|\bar{a}\bar{b}|$;

(3) both electrons on the same orbital, $|a\bar{a}|$ and $|b\bar{b}|$.

In the valence-bond (VB) framework the two first arrangements correspond to neutral determinants, the latter one to ionic ones. The combination of these determinants gives four different configurations:

(a) a neutral singlet state of *g* symmetry, S_g^N,

$$|S_g^N\rangle = (|a\bar{b}| + |b\bar{a}|)/\sqrt{2}; \tag{1}$$

(b) a neutral triplet state of *u* symmetry, T_u^N,

$$|T_u^N\rangle = (|a\bar{b}| - |b\bar{a}|)/\sqrt{2}; \tag{2}$$

(c) an ionic singlet state of *g* symmetry, S_g^I,

$$|S_g^I\rangle = (|a\bar{a}| + |b\bar{b}|)/\sqrt{2}; \tag{3}$$

(d) an ionic singlet state of *u* symmetry, S_u^I,

$$|S_u^I\rangle = (|a\bar{a}| - |b\bar{b}|)/\sqrt{2}. \tag{4}$$

U can be defined as the energy associated with the pairing of two electrons on the same 3*d* orbital,

$$U = E_{|a\bar{a}|} - E_{|a\bar{b}|} \tag{5}$$

and can be written in terms of the energy difference between the ionic and neutral singlet configurations:

$$U = E_{S_g^I} - E_{S_g^N}. \tag{6}$$

So, if we can evaluate the energies of the neutral and ionic states, U can be extracted from their energy difference. However, the energies of these two states cannot be directly obtained from standard quantum chemistry calculations. Since both states belong to the same irreducible symmetry representation, any *ab initio* quantum chemistry calculation will provide solutions where both states are mixed, with different c_I/c_N ratios:

$$^1\Phi_g^1 = c_N|S_g^N\rangle + c_I|S_g^I\rangle,$$

$$^1\Phi_g^2 = c'_N|S_g^N\rangle + c'_I|S_g^I\rangle. \tag{7}$$

Then we need to design a procedure to extract this information from the eigenvalues and eigenvectors of the electronic Hamiltonian. This procedure makes use of the effective Hamiltonian theory, and it has been previously used in the study of magnetic systems, as well as the evaluation of hopping integrals in mixed-valence systems.[29–41] A detailed description of the method can be found in Ref. 41, and a summary enlightening the most striking points will be provided here.

Let us consider a model space $\mathbb{S}$ spanned by the four VB determinants or by their four combinations [Eqs. (1)–(4)]. Its projector is

$$\hat{P}_S = \sum_{i\in S} |\phi_i\rangle\langle\phi_i|. \tag{8}$$

From *ab initio* embedded cluster calculations we can obtain n approximated solutions to the exact Hamiltonian, which hereafter will be considered as exact. These solutions have the largest components in the model space $\mathbb{S}$, $\{\mathbf{\Phi}_k, k=1,n\}$, with energies $\{E_k\}$. They constitute the target space $\mathbb{S}'$. Now we define an effective Hamiltonian in $\mathbb{S}$ such as its n eigenvalues are exact (then equal to $\{E_k\}$) and its eigenvectors are projections of the corresponding exact eigenvectors in the model space. This is the definition of Bloch effective Hamiltonian[42]:

$$\hat{H}_{eff}^{Bloch}|\hat{P}_S\Phi_k\rangle = E_k|\hat{P}_S\Phi_k\rangle. \tag{9}$$

This basic equation leads to the spectral definition of the Bloch effective Hamiltonian[42]:

$$\hat{H}_{eff}^{Bloch} = \sum_{k=1,n} |\hat{P}_S\Phi_k\rangle E_k \langle\hat{P}_S\Phi_k^{\perp}|, \tag{10}$$

where $|\hat{P}_S\Phi_k^{\perp}\rangle$ represents the biorthogonal vector associated with $|\hat{P}_S\Phi_k\rangle$. Actually the projections of the (orthogonal) eigenvectors of $\hat{H}$ onto the model space have in general no reason to be orthogonal. They define an overlap matrix S as follows:

$$S_{ij} = \langle\hat{P}_S\Phi_i|\hat{P}_S\Phi_j\rangle \tag{11}$$

and

$$|\hat{P}_S\Phi_k^{\perp}\rangle = S^{-1}|\hat{p}_S\Phi_k\rangle. \tag{12}$$

The Bloch effective Hamiltonian is non-Hermitian. Its n^2 matrix elements are defined from the n^2 conditions imposed by Eq. (10). In the two-electron/two-orbital problem, n is equal to 4, and the Bloch effective Hamiltonian takes the following form, where the triplet state is the energy origin:

$$\begin{array}{c} |S_g^N\rangle \\ |S_g^I\rangle \\ |T_u^N\rangle \\ |S_u^I\rangle \end{array} \begin{pmatrix} 2K_{ab} & 2t'_{ab} & 0 & 0 \\ 2t_{ab} & U+2K_{ab} & 0 & 0 \\ 0 & 0 & 0 & 0 \\ 0 & 0 & 0 & U+2(K_{ab}-K'_{ab}) \end{pmatrix}, \tag{13}$$

where K_{ab} and K'_{ab} are the exchange integrals:

$$K_{ab} = \langle a\bar{b}|H_{eff}^{Bloch}|b\bar{a}\rangle,$$

$$K'_{ab} = \langle a\bar{a}|H_{eff}^{Bloch}|b\bar{b}\rangle, \tag{14}$$

and t_{ab} and t'_{ab} the hopping integrals between centers a and b:

$$t_{ab} = \langle a\bar{b}|H_{eff}^{Bloch}|a\bar{a}\rangle,$$

$$t'_{ab} = \langle a\bar{a}|H_{eff}^{Bloch}|a\bar{b}\rangle. \tag{15}$$

The differences between K_{ab} and K'_{ab} and t_{ab} and t'_{ab} result from the nonhermiticity of the Bloch Hamiltonian. The hermiticity can be restored by means of the des Cloizeaux[43] or Gram-Schmidt[44] procedures, based on the orthogonalization of the projections of the eigenvectors on the model space.

It is worth to notice that this procedure requires the knowledge of four states. The neutral ones are in most of the cases the lowest states in their symmetry, but the ionic ones are excited states. For those cases where the excited ionic states cannot be unambiguously determined or they are strongly contaminated by other configurations such as ligand-to-metal charge transfer excitations, the use of an intermediate effective Hamiltonian,[45] instead of the procedure described above, is more pertinent. The intermediate Hamiltonian is built on a four dimensional model space but it is only asked to reproduce the energies of the neutral singlet and triplet states and projections of the singlet state onto the model space (c_I and c_N coefficients). It is possible to demonstrate that the on-site Coulomb repulsion on this scheme is equal to[41]

$$U^{int} = 2t_{ab}\frac{c_I^2 - c_N^2}{c_I c_N}, \tag{16}$$

where t_{ab} keeps the valence value. This approach is reasonable since t_{ab} is only moderatly dependent on the electronic correlation as it has been shown in the past for several authors in quite different systems.[33,37–39,41,46–51]

2. Physical model

A bulk fragment of formula Ti_2O_{10} has been chosen to evaluate U. It is composed of two Ti atoms and the nearest neighbor oxygen atoms. The remainder of the crystal is represented by means of a set of point charges, which approximately reproduce the Madelung potential of the infinite crystal. In order to avoid an artificial polarization of the electrons of the cluster, the Ti atoms in the immediate surroundings of the cluster are represented by total ion potentials (TIPs) (Fig. 1). The geometries of all the atoms are obtained from a previous periodic density functional theory (DFT) calculation carried on the bulk of TiO_2 rutile,[52] which correctly reproduces the experimental lattice parameters. Notice that this fragment contains two extra electrons, resulting from the removal of an oxygen atom on the surface or any other chemical process such as the deposition of a donor atom or molecule such as an alkali metal. In order to take into account the effect on the U value of the geometrical relaxations induced by these extra electrons, partial geometry optimizations have also been carried out. Details of them are provided on next section.

Three sets of basis functions have been employed. Oxygen atoms are represented by means of an ANO-L-type basis functions with a contraction $(4s3p1d)$.[53] For Ti atoms, the core electrons are replaced by pseudopotentials. We deal with 12 valence electrons when the pseudopotential and basis set proposed by Hay and Wadt[54] are used (basis 1) and 10 valence electrons if Barandiarán and Seijo's set is employed,[55] with a $(3s3p4d)$ contraction scheme (basis 2). Finally, basis 3 consists of Hay and Wadt representation for Ti atoms, and ANO-L-type basis functions with an additional d shell for oxygen atoms [contraction $(4s3p2d)$].

Regarding the embedding, several choices are possible for the values of the point charges. There is a general consensus with respect to the partial covalent character of TiO_2 at difference with other systems extensively used in *ab initio* embedded cluster calculations such as MgO.[56,57] For this reason a completely ionic representation for this system could be not adequate.[58,59] In order to check the impact of the environment representation on the U value, we have used two different models for the embedding:

(a) Model 1: a fully ionic representation, with charges {+4} and {−2} for Ti and O atoms, respectively, (model 1);

(b) Model 2: a completely covalent representation, with charges {+2} and {−1}, (model 2).

The bare cluster, with only TIPs in the neighborhood, gives meaningless results, as expected, due to a significant contamination of the ionic states, which impedes us a univocal characterization of the ionic states. On the other hand, as will be shown below, the effect on the U value of the representation used to model the crystal is practically negligible.

3. Approximation to the exact N-electron wave functions

Highly correlated N-electron wave functions are obtained from state-of-the-art quantum chemistry techniques. The on-site repulsion is evaluated from the energies and wave functions obtained from three CI spaces:

(a) The bare valence complete active space (CAS), that is a CASCI space.

(b) The CAS+S space, including all the single excitations on the top of the active space. This expansion includes three types of determinants:

(1) $1h$, where an electron moves from an inactive occupied orbital to an active orbital;

(2) $1p$, where an electron moves from an active to an inactive virtual orbital; and

(3) $1h+1p$, where an electron moves from an occupied to a virtual orbital.

It is worth to note that these excitations can be coupled with simultaneous single excitations inside the active space.

(c) The DDCI space, acronym of difference dedicated CI space,[60] where all the single and double excitations on the top of the CAS are included in the CI calculations, except those which do not involve an active orbital. Thus, a double excitation from two inactive occupied orbitals to two virtual ones is not included in the calculation. While these excluded excitations, which are the most numerous, contain the most part of the electronic correlation energy, they do not contribute to the energy difference among the states involved in the evaluation of U. So, the use of the DDCI approach considerably reduces the computational cost with respect to single and double configuration interaction (SDCI) calculations, but it assures the introduction of the component of the correlation energy which plays a differential role in the stabilization of the states under study. This strategy has been extensively used in the recent past, especially in the evaluation of magnetic coupling constants as well as the determination of hopping integrals in numerous systems.[29–41,46,48,49,61,62]

The whole procedure can be summarized as follows.

(1) A fragment of the bulk structure of TiO_2 has been chosen, containing two neighbor Ti centers, and the ten oxygen atoms around them, as shown in Fig. 1. This cluster is embedded in a set of point charges which model the effect of the Madelung potential of the infinite crystal on the centers of the cluster. This cluster is doped with two extra electrons, representing the effect of the reduction which takes place somewhere in the crystal surface.

(2) Accurate *ab initio* embedded cluster CI calculations have been performed over a complete active space (CAS) composed by two electrons and the two $3d$ orbitals. These calculations provide the four states $({}^3\Phi_u, {}^1\Phi_u, {}^1\Phi_g^1, {}^1\Phi_g^2)$ with largest projections on the model space. These four states constitute the target space. The projections of the eigenvectors ${}^3\Phi_u$ and ${}^1\Phi_u$ onto the model space are fixed by symmetry. It is not the case for the singlet states ${}^1\Phi_g^1$ and ${}^1\Phi_g^2$ whose projections in the model space have a degree of freedom, namely, the ratio of the coefficients on S_g^N and S_g^I (c_I and c_N). From the energies of these four states and the ratios of the coefficients c_I/c_N we can univocally fix the values of the five parameters on the Bloch Hamiltonian [Eq. (13)]. The Gram-Schmidt procedure is less demanding, as it only requires the energies of these four states and the ratio c_I/c_N of the ground ${}^1\Phi_g^1$ state.

(3) For all the DDCI calculations, where ionic states are too high in energy, we use the intermediate effective Hamiltonian theory and U is evaluated from the projection of the singlet state on the model space as shown in Eq. (16).

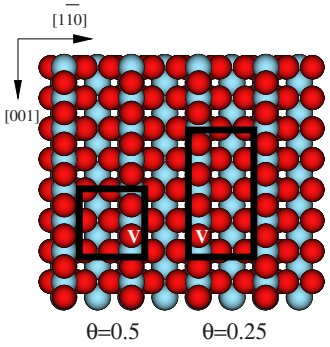

FIG. 2. (Color online) Schematic representation of the two cells employed in periodic calculations: the 2×1 (on the left) and 4×1 (on the right) cells, corresponding to vacancy concentrations of $\theta=0.5$ and $\theta=0.25$, respectively. "V" represents the bridging oxygen vacancy.

B. LDA+U calculations

Once an estimate of the U value is obtained from our *ab initio* embedded cluster calculations, we proceed to the study of reduced (110) TiO_2 surface by means of periodic DFT calculations. The calculations were performed using the projected augmented wave approach[63] and the VASP4.6 code,[64–66] with a cutoff for the plane waves of 500 eV. The electrons explicitly included in the calculations are the $3p$, $4s$, and $3d$ shells of Ti and the $2s$ and $2p$ shells of O.[67,68] For k-point sampling we used the lowest order Monkhorst-Pack[69] set of $4\times4\times1$ k points, including the Γ point. The LSDA+U approximation introduced by Dudarev *et al.*[24] was used, where our U value is equivalent to the U_{eff} parameter ($U_{eff}=U-J$) proposed by these authors.

To describe the TiO_2 (110) rutile surface a slab model is used. The slabs are obtained through replication along the three directions of a supercell that includes a portion of vacuum. The reduced surfaces are finally modeled by removing oxygen atoms from the bridge positions which have been experimentally established as the most stable vacancies.[1,70–72]

Two different vacancy concentrations have been considered: $\theta=0.25$ and $\theta=0.5$, where θ represents the mean number of oxygen vacancies per surface unit cell. The corresponding unit cells are composed of one primitive surface unit cell in the $[1\bar{1}0]$ direction and four ($\theta=0.25$) or two ($\theta=0.50$) primitive surface unit cells in the [001] direction, as schematically shown in Figs. 2 and 5. Regarding the slab thickness, it has been argued by one of us[52] that energies are almost converged at the GGA level for those calculations using at least a five-layer slab. Assuming a similar behavior for LDA+U calculations, we keep the slab thickness in five layers, the analysis of the influence of the slab on the position of the band-gap state being outside the scope of this work. The notations used hereafter for the resulting super cells are (2×1) and (4×1) for vacancy concentrations $\theta=0.5$ and $\theta=0.25$, respectively.

We perform spin polarized calculations on the triplet spin state, as suggested by previous works.[22,23] The starting geometries are those obtained for the relaxed surface after oxygen removal from GGA periodic calculations by Oviedo *et al.*,[52] and then we perform geometry optimizations in order to analyze the dependence of the band-gap states on the atomic structure, as recently suggested by Di Valentin *et al.*[23] for the hydroxylated TiO_2 (110) surface. These authors have found a close relationship between a correct structural relaxation and the occurrence of electron trapping, when hybrid exchange functionals are used. For each considered U value, geometry optimizations have been carried out, maintaining the atoms in the two bottom layers fixed at their original positions, until the largest energy difference between two successive points was less than 1×10^{-3} eV.

TABLE I. U values (eV) obtained with different environment representations and several CI wave functions.

Model	Basis set	CAS+S Bloch	CAS+S Gram-Schmidt	DDCI Int.
(+4,−2) Model 1	1	5.80	5.84	6.16
	2	5.63	5.66	6.39
	3	5.43	5.47	5.54
(+2,−1) Model 2	1	5.37	5.45	5.95
	2	5.56	5.63	6.48
	3	4.93	5.02	5.24
Mean $\bar{U}$ values		5.45	5.51	5.96

III. RESULTS

A. *Ab initio* evaluation of U

The U values obtained from *ab initio* calculations are reported in Table I. We have analyzed (i) the effect of the electronic correlation, (ii) the dependency on the basis sets, and (iii) the impact of the environment model on the U value. Also the effect of the geometrical relaxation induced by the extra electrons on the U value is discussed in this section.

As shown in Table I, both the basis sets and the environment have a minor effect on the U values, at least for the accuracy demanded for the subsequent periodic calculations, as discussed below. Only the electronic correlation plays an important role, and we focus the discussion on its effect on the U value.

Regarding the impact of the wave function complexity, in all cases the U values obtained from the bare valence space are extremely large (U values around 13–14 eV), due to an artificial destabilization of the ionic states. A remarkable decrease of the U value is observed when the single excitations are included in the CI expansion (CAS+S results in Table I). This important modification of U is due to the dynamical polarization of the ionic forms, which is introduced by the $1h+1p$ determinants. The rest of contributions included in the DDCI space produce a minor modification of U. This result suggests that for those systems where the DDCI calculation is not available, a reasonable U value could be ob-

tained at the CAS+S level, at a remarkable lower computational cost. The same general trend has been found in the recent past for several magnetic binuclear Cu(II) systems, where U is essentially affected by the single excitations, the double excitations producing only a minor change.[41]

At the CAS+S level, both Bloch and Gram-Schmidt U values are very close, independently of the basis sets and representation of the environment. This means that the nonhermiticity inherent to the Bloch approach does not affect the U value (while it changes significantly the hopping integrals t, for instance). The mean U value obtained at this level is around 5.5 eV. However, for the CAS+S solutions, the agreement with the intermediate U values is not so good (differences as large as 1.5 eV are found). The comparison with previous works on different systems[41] revels that U values provided by the intermediate Hamiltonian are always larger than those coming from Bloch or Gram-Schmidt Hamiltonians. The simplifications inherent to the intermediate Hamiltonian produce an enhancement of the U value, especially for low-level wave functions, such as CAS+S ones, where the c_I/c_N ratio of the ground $^1\Phi_g^1$ state is underestimated with respect to the DDCI wave function. The differences are not so pronounced for DDCI solutions, although the same trend is observed. In spite of this limitation, it is worth to notice that the procedure based on the use of intermediate Hamiltonian is the only one available for those systems where there exists a large contamination of the ionic states (that prevents a correct identification of the excited states) or those with a large number of low-lying ligand-to-metal charge transfer excitations. Then, the DDCI values reported in Table I, which have been obtained by means of the intermediate Hamiltonian approach, must be considered as an upper limit of the U parameter.

An additional aspect of the method used concerns whether the active space employed on the CI calculations is large enough to evaluate U. In order to analyze the suitability of the active space we have determined the singlet-triplet energy difference by means of CAS self-consistent field calculations. We have compared the results obtained when an enlarged CAS containing two active electrons and ten moleculor orbitals (MOs) with large Ti 3d character is employed with those coming from a minimal CAS (two electrons in two 3d MOs). The so-calculated singlet-triplet gaps differ by less than 1 meV. Indeed, the enlarged CAS wave functions are significantly dominated by the configurations contained in the minimal CAS (projections larger than 98%). The same negligible effect is observed when the active space contains also molecular orbitals centered on the ligands [CAS (12MOs/6e)]. These results support the use of a minimal active space in our extended CI calculations.

Finally, the effect of the geometry relaxation on the U value has been addressed. It is expected that the extra electrons induce a relaxation not only on the first neighbor atoms to the two Ti centers, but also to the second and perhaps third coordination spheres. However, a full geometry optimization on an extended cluster, containing several Ti centers is meaningless in the present case because, as discussed in previous section, the theoretical evaluation of U requires a wave function distributing two electrons in two neighbor Ti sites. It has been observed that when an extended cluster is employed, the ground state corresponds to two electrons located in noncontiguous positions. This situation probably represents the most stable electronic distribution in the real system, but it is useless for our purposes, since it introduces the geometrical relaxation in quite distant Ti positions and not in two neighbor Ti centers as desired. On the other hand, a full optimization of the Ti_2O_{10} cluster is not possible, due to the frozen positions of the total ion potentials and point charges. The nearest neighborhood of the cluster is not affected by the relaxation, which produces unrealistic final geometries. For the above reasons, we have estimated the impact of the geometrical relaxation on the U value from a series of test calculations, in which a progressive breathing expansion of the Ti_2O_{10} cluster is allowed, as well as the nearest neighbor atoms. The breathing of the cluster enlarges the Ti-Ti distance and leads to a stabilization of the neutral configuration, while the ionic ones are practically unaffected. Then the ionic-neutral energy difference, i.e., U term, increases. Even though significant changes in the total energy of the system are observed, the U value increases by no more than 10% with respect to the original geometry.

In summary, our *ab initio* calculations suggest a U value around 5.5±0.5 eV for reduced TiO_2. This value is in agreement with those extracted from XPS and EELS experiments ranging from 4 to 5 eV.[57,73–75]

B. Periodic LDA+U calculations

The density-of-states (DOS) curves obtained from our LDA+U calculations are depicted in Fig. 3 for the 2×1 unit cell. We have employed several values of U in the LDA+U calculations, in order to check the sensibility of the periodic approach to the U value used and to discard a fortuitous agreement between the *ab initio* U value and the U value which provides a correct description of the band-gap states at the LDA+U level. The aim is not to suggest a U value based on empirical fitting of the band-gap states, but to test the capabilities of the strategy proposed. The left panels in Fig. 3 show the DOS curves obtained at the LDA+U level with GGA optimized structures. The right panels report the DOS curves obtained when also the geometry is optimized at the LDA+U level. As usual for DFT calculations,[76] the band gap is underestimated for all the U values considered (band gap around 2.2 eV instead of 3.1 eV).[3] As far as we know among DFT based approaches only the hybrid B3LYP functional gives a better agreement to the band-gap energy, although slightly overestimated (3.4 eV).[23] Examination of DOS reveals that for $U=0$ the Ti 3d-like surface state lays in the conduction band, as previously reported.[20,21]

For U values ranging from 5 to 7 eV, there are localized states on the band gap. In contrast to the B3LYP calculations of Di Valentin *et al.*,[23] these states appear both when the GGA relaxed surface is used as well as when the geometry optimization is performed at the LDA+U level, probably due to the effect of the U term. However, the *position* of these states is quite dependent on the precise structural relaxation carried out, even when changes in Ti-Ti distances once the optimization has been completed never exceed 0.06 Å. As a general trend, in all cases, the electron trapping states move

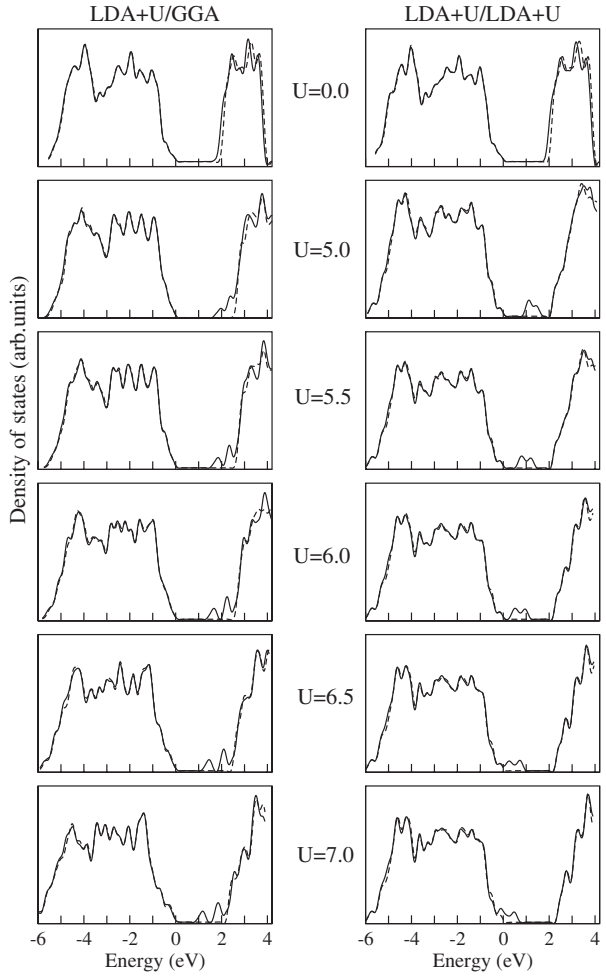

FIG. 3. Density-of-states curves obtained from LDA+U calculations with different values of U using the 2×1 cell (vacancy concentration $\theta=0.5$). The zero of energy corresponds to the valence-band edge. Left panel: LDA+U energies with GGA optimized geometry (LDA+U/GGA). Right panel: the geometry is also optimized by using the LDA+U approach (LDA+U/LDA+U). Solid and dashed lines correspond, respectively, to the majority and minority spin components.

toward the valence-band edge. This is an important point to be considered in future applications of the LDA+U procedure, since so far most of the published LDA+U studies of transition metal oxides where U values are fitted in an empirical way does not take into account the possible effects of the specific structural relaxation introduced for each U value.

For the suggested U value (5.5 ± 0.5 eV) two distinct peaks are observed in the density of states, 0.88 and 1.27 eV below the conduction-band edge for the LDA+U optimized geometry, which nicely correlate with the experimental data. For U larger than 6.0 eV, the localized states are placed in the lower part of the band gap, close to the valence-band edge. Even when it could be possible to relate these states to the broad peaks observed in the region of 450–750 nm for irradiated rutile,[11–14] the controversy regarding their assignment impedes us from doing. For $U=8$ eV and higher, the band gap disappears, the valence-band edge mixes with the bottom of the conduction band.

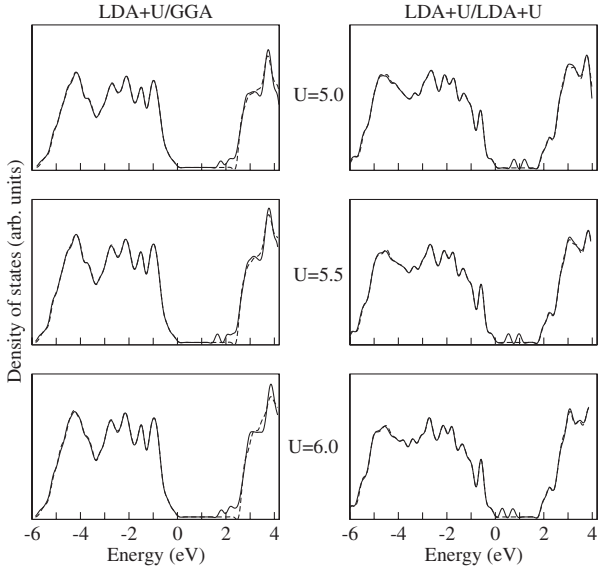

FIG. 4. Density-of-states curves obtained from LDA+U calculations with three different U values for a vacancy concentration of 0.25 (4×1 cell). The zero of energy corresponds to the valence-band edge. Left panel: LDA+U energies with GGA optimized geometry (LDA+U/GGA). Right panel: the geometry is also optimized by using the LDA+U approach (LDA+U/LDA+U). Solid and dashed lines correspond, respectively, to the majority and minority spin components.

Figure 4 presents the DOS curves obtained for a lower vacancy concentration ($\theta=0.25$) when U values on the range provided by the *ab initio* calculations are used. As for $\theta=0.5$, the positions of the band-gap states are affected by the geometrical relaxation, but a nice agreement with experimental data is found for the *ab initio* U value. A closer inspection of Figs. 3 and 4 reveals that the gap states move toward the conduction-band edge as the defect concentration increases (defect states lie at 0.54 and 0.98 eV above the valence-band edge for a $\theta=0.25$ vacancy concentration, which move to 0.80 and 1.19 eV when $\theta=0.50$) in agreement with UPS measurements.[77,78] The inset of Fig. 5 shows this effect in detail. The curves in this figure correspond to the total density of states obtained for the 2×1 (thin line) and 4×1 (solid line) cells from LDA+U calculations, with $U=5.5$ eV on the LDA+U optimized geometry.

In order to clarify the composition of the band-gap states and the impact of the geometry relaxation on their localized nature, we obtain the projection of the DOS (PDOS) on the Ti atoms for both cells, shown in Fig. 5 (middle panel: 2×1 cell; bottom panel: 4×1 cell) for the GGA (left) and LDA+U (right) relaxed geometries ($U=5.5$ eV). For the LDA+U geometry, the band-gap states are essentially centered in two specific Ti atoms in both cells, but with different nature depending on the vacancy concentration. For low concentrations, the electrons trap on subsurface Ti atoms, while for high concentrations, half of the electrons localizes on subsurface Ti atoms, the rest on surface Ti atoms, close to the oxygen defect. The relationship between vacancy concentration and Ti^{+3} distribution could affect the catalytic activity of the material, and even play a crucial role on subsequent ap-

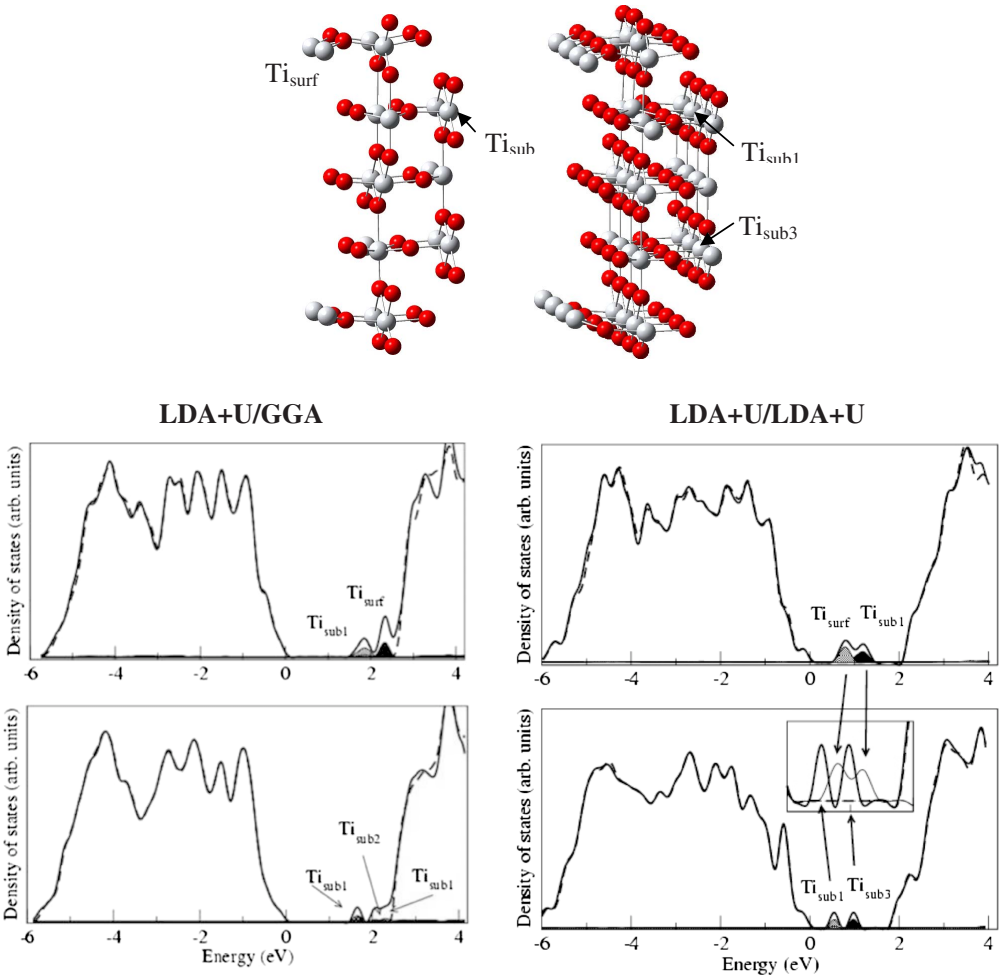

FIG. 5. (Color online) Total and projected density of states for reduced TiO_2 (110), with two different vacancy concentrations $\theta=0.5$ (middle panel) and $\theta=0.25$ (bottom panel), calculated using the LDA+U method on the GGA geometry (left) or on the relaxed LDA+U geometry (right). In all cases a value of $U=5.5$ eV has been employed. On the top: the five-layer slabs used in the calculations (left, vacancy concentration: $\theta=0.5$; right, vacancy concentration: $\theta=0.25$). The Ti^{+3} states are localized on surface and subsurface Ti ions for $\theta=0.5$ and only subsurface Ti ions for $\theta=0.25$. The inset shows how the increase of the vacancy concentration θ pushes the band-gap states toward the conduction-band edge for the LDA+U geometry. Solid and dashed lines correspond, respectively, to the majority and minority spin components.

plications. It is worth to mention that it could be possible to conceive several localized solutions with approximately the same energy, but in all of our calculations, independently of both the U used and the starting spin configuration, we obtain the Ti^{+3} distribution described above, and we have not found an alternative way to converge over different solutions.

Regarding the effect of the lattice relaxation, the comparison of the PDOS obtained from the GGA and LDA+U geometries indicates that the localized nature of these states is strongly related with the relaxation effects induced by the extra electrons. When the GGA geometry is used the band-gap states present a lower Ti $3d$ character (smaller projections on the Ti atoms), and larger delocalization, especially for low vacancy concentration, where only one of the band-gap states is well separated from the conduction band.

IV. CONCLUSIONS

The failure of LDA based methods in describing the transition metal oxide surfaces has motivated the development of alternative methods able to deal with electron correlation effects. Among those methods, LDA+U approach is a promising one, the main limitation is that U is generally considered as an empirical parameter to be fixed during the calculations.

In this context, a general protocol to estimate a reasonable value of U to be injected in the LDA+U calculations has been presented here, and illustrated in the case of reduced (110) rutile surface.

The procedure provides a U value of 5.5 ± 0.5 eV, which once introduced in the LDA+U calculations gives a correct description of the band-gap states. The $3d$ character of these states is confirmed and the effect of the vacancy concentra-

tion on the relative position is also reproduced. Moreover, our results show a strong dependence between the position of the band-gap states and the approach used to account for the lattice relaxation, with marked differences between the DOS obtained from LDA+U calculations using the optimal GGA geometry or the corresponding relaxed LDA+U structure.

So, the procedure is quite promising, and can be considered as an alternative tool for those systems where electronic correlation plays a crucial role, and LDA+U descriptions could help in understanding their properties.

ACKNOWLEDGMENTS

This work was funded by the Spanish DGESIC, Project No. MAT2005-1872. N.C.H. thanks the Ramón y Cajal Program from Spanish Ministerio de Ciencia y Tecnología.

*Author to whom correspondence should be addressed. FAX: +34-954-557174. calzado@us.es

[1] U. Diebold, Surf. Sci. Rep. **48**, 53 (2003).
[2] V. E. Henrich and P. A. Cox, *The Surface Science of Metal Oxides* (Cambridge University Press, Cambridge, 1994).
[3] V. E. Henrich and R. L. Kurtz, Phys. Rev. B **23**, 6280 (1981).
[4] Y. Aiura, Y. Nishihara, Y. Haruyama, T. Komeda, S. Kodaira, Y. Sakisaka, T. Maruyama, and H. Kato, Physica B **196**, 1215 (1994).
[5] Z. Zhang, S. P. Jeng, and V. E. Henrich, Phys. Rev. B **43**, 12004 (1991).
[6] R. Heise, R. Courths, and S. Witzel, Solid State Commun. **84**, 599 (1992).
[7] U. Diebold, H. S. Tao, N. D. Shinn, and T. E. Madey, Phys. Rev. B **50**, 14474 (1994).
[8] W. Göpel, J. A. Anderson, D. Frankel, M. Jaehnig, K. Phillips, J. A. Schäfer, and G. Rocker, Surf. Sci. **139**, 333 (1984).
[9] M. A. Henderson, Surf. Sci. **400**, 203 (1998).
[10] D. C. Cronemeyer, Phys. Rev. **113**, 1222 (1959).
[11] W.-T. Kim, C.-D. Kim, and Q. W. Choi, Phys. Rev. B **30**, 3625 (1984).
[12] A. K. Ghosh, F. G. Wakim, and R. R. Addiss, Phys. Rev. **184**, 979 (1969).
[13] T. Asahi, A. Furube, and H. Masuhara, Chem. Phys. Lett. **275**, 234 (1997).
[14] K. R. Gopidas, M. Bohorquez, and P. V. Kamat, J. Phys. Chem. **94**, 6435 (1990).
[15] M. A. Henderson, W. S. Epling, C. H. F. Peden, and C. L. Perkins, J. Phys. Chem. B **107**, 534 (2003).
[16] A. K. See and R. A. Bartynski, J. Vac. Sci. Technol. A **10**, 2591 (1992).
[17] I. Justicia, P. Ordejón, G. Canto, J. L. Mozos, J. Fraxedas, G. A. Battiston, R. Gerbasi, and A. Figueras, Adv. Mater. (Weinheim, Ger.) **14**, 1399 (2002).
[18] B. O'Regan and M. Grätzel, Nature (London) **353**, 737 (1991).
[19] M. K. Nazeeruddin, A. Kay, I. Rodicio, R. Humphry-Baker, E. Müller, P. Liska, N. Vlachopaulos, and M. Grätzel, J. Am. Chem. Soc. **115**, 6383 (1993).
[20] M. Ramamoorthy, D. Vanderbilt, and R. D. King-Smith, Phys. Rev. B **49**, 16721 (1994).
[21] A. T. Paxton and L. Thiên-Nga, Phys. Rev. B **57**, 1579 (1998).
[22] P. J. D. Lindan, N. M. Harrison, M. J. Gillan, and J. A. White, Phys. Rev. B **55**, 15919 (1997).
[23] C. Di Valentin, G. Pacchioni, and A. Selloni, Phys. Rev. Lett. **97**, 166803 (2006).
[24] S. L. Dudarev, G. A. Botton, S. Y. Savrasov, C. J. Humphreys, and A. P. Sutton, Phys. Rev. B **57**, 1505 (1998).
[25] C. Loschen, J. Carrasco, K. M. Neyman, and F. Illas, Phys. Rev. B **75**, 035115 (2007).
[26] M. Cococcioni and S. de Gironcoli, Phys. Rev. B **71**, 035105 (2005).
[27] S. Fabris, S. de Gironcoli, S. Baroni, G. Vicario, and G. Balducci, Phys. Rev. B **71**, 041102(R) (2005).
[28] D. A. Scherlis, M. Cococcioni, P. Sit, and N. Marzari, J. Phys. Chem. B **111**, 7384 (2007).
[29] C. J. Calzado and J. P. Malrieu, Phys. Rev. B **63**, 214520 (2001).
[30] C. J. Calzado and J. P. Malrieu, Eur. Phys. J. B **21**, 375 (2001).
[31] J. Cabrero, C. J. Calzado, D. Maynau, R. Caballol, and J. P. Malrieu, J. Phys. Chem. A **106**, 8146 (2002).
[32] I. de P. R. Moreira and F. Illas, Phys. Chem. Chem. Phys. **8**, 1645 (2006).
[33] E. Bordas, C. de Graaf, R. Caballol, and C. J. Calzado, Phys. Rev. B **71**, 045108 (2005).
[34] E. Bordas, R. Caballol, C. de Graaf, and J. P. Malrieu, Chem. Phys. **309**, 259 (2005).
[35] C. de Graaf, L. Hozoi, and R. Broer, J. Chem. Phys. **120**, 961 (2004).
[36] C. J. Calzado, C. de Graaf, E. Bordas, R. Caballol, and J. P. Malrieu, Phys. Rev. B **67**, 132409 (2003).
[37] N. Suaud, A. Gaita-Ariño, J. M. Clemente-Juan, and E. Coronado, Chem.-Eur. J. **10**, 4041 (2004).
[38] N. Suaud, A. Gaita-Ariño, J. M. Clemente-Juan, J. Sánchez-Marín, and E. Coronado, Polyhedron **22**, 2331 (2003).
[39] N. Suaud, A. Gaita-Ariño, J. M. Clemente-Juan, J. Sánchez-Marín, and E. Coronado, J. Am. Chem. Soc. **124**, 15134 (2002).
[40] C. J. Calzado, J. Cabrero, J. P. Malrieu, and R. Caballol, J. Chem. Phys. **116**, 2728 (2002).
[41] C. J. Calzado, J. Cabrero, J. P. Malrieu, and R. Caballol, J. Chem. Phys. **116**, 3985 (2002).
[42] C. Bloch, Nucl. Phys. **6**, 329 (1958).
[43] J. des Cloizeaux, Nucl. Phys. **20**, 321 (1960).
[44] See, for instance, W. H. Press, B. P. Flannery, S. A. Teukolsky, and W. T. Vetterling, *Numerical Recipes* (Cambridge University Press, Cambridge, 1986).
[45] J. P. Malrieu, P. Durand, and J. P. Daudey, J. Phys. A **18**, 809 (1985).
[46] C. J. Calzado, J. P. Malrieu, and J. F. Sanz, J. Phys. Chem. A **102**, 3659 (1998).
[47] J. F. Sanz, C. J. Calzado, and A. Márquez, Int. J. Quantum Chem. **76**, 458 (2000).
[48] C. J. Calzado, J. F. Sanz, and J. P. Malrieu, J. Chem. Phys. **112**, 5158 (2000).
[49] C. J. Calzado and J. P. Malrieu, Chem. Phys. Lett. **317**, 404 (2000).

[50] L. A. Curtiss and J. R. Miller, J. Phys. Chem. A **102**, 160 (1998).
[51] K. Kim, K. D. Jordan, and M. N. Paddon-Row, J. Phys. Chem. **98**, 11053 (1994).
[52] J. Oviedo, M. A. San Miguel, and J. F. Sanz, J. Chem. Phys. **121**, 7427 (2004).
[53] P. O. Widmark, P. A. Malmqvist, and B. O. Ross, Theor. Chim. Acta **77**, 291 (1990).
[54] P. J. Hay and W. R. Wadt, J. Chem. Phys. **82**, 299 (1985).
[55] Z. Barandiarán and L. Seijo, Can. J. Chem. **70**, 409 (1992).
[56] C. Sousa and F. Illas, Phys. Rev. B **50**, 13974 (1994).
[57] A. E. Bocquet, T. Mizokawa, K. Morikawa, A. Fujimori, S. R. Barman, K. Maiti, D. D. Sarma, Y. Tokura, and M. Onoda, Phys. Rev. B **53**, 1161 (1996).
[58] T. Bredow, E. Aprà, M. Catti, and G. Pachioni, Surf. Sci. **418**, 150 (1998).
[59] T. Bredow and G. Pachioni, Surf. Sci. **426**, 106 (1999).
[60] J. Miralles, O. Castell, R. Caballol, and J. P. Malrieu, Chem. Phys. **172**, 33 (1993).
[61] C. J. Calzado, J. F. Sanz, J. P. Malrieu, and F. Illas, Chem. Phys. Lett. **307**, 102 (1999).
[62] I. de P. R. Moreira, F. Illas, C. J. Calzado, J. F. Sanz, J. P. Malrieu, N. B. Amor, and D. Maynau, Phys. Rev. B **59**, R6593 (1999).
[63] M. C. Payne, M. P. Teter, D. C. Allan, T. A. Arias, and J. D. Joannopoulos, Rev. Mod. Phys. **64**, 1045 (1992).
[64] G. Kresse and J. Hafner, Phys. Rev. B **47**, 558 (1993).
[65] G. Kresse and J. Furthmüller, Comput. Mater. Sci. **6**, 15 (1996).
[66] G. Kresse and J. Furthmüller, Phys. Rev. B **54**, 11 169 (1996).
[67] P. E. Blöchl, Phys. Rev. B **50**, 17953 (1994).
[68] G. Kresse and D. Joubert, Phys. Rev. B **59**, 1758 (1999).
[69] H. Monkhorst and J. Pack, Phys. Rev. B **13**, 5188 (1976).
[70] U. Diebold, J. Lehman, T. Mahmoud, M. Kuhn, G. Leonardelli, W. Hebenstreit, M. Schmid, and P. Varga, Surf. Sci. **411**, 137 (1998).
[71] E. L. D. Hebenstreit, W. Hebenstreit, and U. Diebold, Surf. Sci. **461**, 87 (2000).
[72] E. L. D. Hebenstreit, W. Hebenstreit, and U. Diebold, Surf. Sci. **470**, 347 (2001).
[73] K. Okada, T. Uozumi, and A. Kotani, J. Phys. Soc. Jpn. **63**, 3176 (1994).
[74] T. Uozumi, K. Okada, and A. Kotani, J. Phys. Soc. Jpn. **62**, 2595 (1993).
[75] A. Tanaka and T. Jo, J. Phys. Soc. Jpn. **63**, 2788 (1994); T. Jo and A. Tanaka, *ibid.* **64**, 676 (1994).
[76] J. Heyd and G. E. Scuseria, J. Chem. Phys. **121**, 1187 (2004).
[77] V. E. Henrich, G. Dresselhaus, and H. J. Zeiger, Phys. Rev. Lett. **36**, 1335 (1976).
[78] H. R. Sadeghi and V. E. Henrich, J. Catal. **109**, 1 (1988).